The Journal of Chemical Physics

# Dependence of effective desorption kinetic parameters on surface coverage and adsorption temperature: CO on Pd(111)

Cite as: J. Chem. Phys. **90**, 6761 (1989); https://doi.org/10.1063/1.456294
Submitted: 27 January 1989 • Accepted: 16 February 1989 • Published Online: 31 August 1998

**Xingcai Guo and John T. Yates**


View Online


Export Citation

**ARTICLES YOU MAY BE INTERESTED IN**

CO adsorption on Pd(111) and Pd(100): Low and high pressure correlations
Journal of Vacuum Science & Technology A **11**, 1969 (1993); https://doi.org/10.1116/1.578532

A molecular beam investigation of the catalytic oxidation of CO on Pd (111)
The Journal of Chemical Physics **69**, 1267 (1978); https://doi.org/10.1063/1.436666

Adsorption of CO on Pd(100)
The Journal of Chemical Physics **73**, 2984 (1980); https://doi.org/10.1063/1.440430

Lock-in Amplifiers up to 600 MHz
Zurich Instruments
Watch




© 1989 American Institute of Physics.

# Dependence of effective desorption kinetic parameters on surface coverage and adsorption temperature: CO on Pd(111)

Xingcai Guo and John T. Yates, Jr.
*Surface Science Center, Department of Chemistry, University of Pittsburgh, Pittsburgh, Pennsylvania 15260*

(Received 27 January 1989; accepted 16 February 1989)

The effective desorption kinetic parameters of CO on the Pd(111) surface have been studied by thermal desorption spectroscopy. The zero coverage effective desorption activation energy and the preexponential factor were found to be 35.5 kcal/mol and $10^{13.5}$ $s^{-1}$, respectively. As a function of CO coverage, a four-stage correlation between $E_d(\theta)$ and the development of stable low-energy electron desorption (LEED) structures was observed for the first time at $T_{ads} = 200$ K. $E_d$ and $\nu_1$ showed a strong compensation effect with $T_c = 519$ K. The adsorption temperature dependence of $E_d$ from $T_{ads} = 87$ to 200 K was observed and interpreted qualitatively by a model involving the production of different domain structures at various adsorption temperatures and the preservation of domain structures at higher coverages during temperature programmed desorption.

## I. INTRODUCTION

Thermal desorption is a very important process (the final step) in heterogeneously catalyzed surface reactions. The desorption rate from a surface has been conventionally modeled by the Polanyi–Wigner equation[1]

$$-\frac{d\theta}{dt} = \nu_n \theta^n \exp(-E_d/RT), \quad (1)$$

where $\theta$ is the fractional surface coverage, $n$ the desorption order, $E_d$ the desorption activation energy, and $\nu_n$ the preexponential factor. It has been shown that for desorption from single crystal surfaces $E_d$ and $\nu_n$ are not constant in many cases, but vary with surface coverage.[2] This often occurs because of the adsorbate lateral interactions (attractive or repulsive) which may lead to multiple binding states. Therefore, the variation of these desorption kinetic parameters with coverage may reflect the changes of the adsorbate structure. In this paper, we will demonstrate this relationship by studying CO desorption from the Pd(111) surface. We will also report the dependence of $E_d$ and $\nu_n$ on the adsorption temperature, which has not been examined before.

The CO/Pd(111) system has been extensively studied previously with various methods.[3] Some of the results are summarized in Fig. 1. CO is molecularly bonded to the Pd(111) surface through the C atom. The saturation coverage is 0.66 at $T_{ads} = 200$ K[4] and 0.75 at $T_{ads} = 90$ K.[5] As the CO coverage increases, a sequence of LEED patterns is observed[4,5]: $(\sqrt{3}\times\sqrt{3})R\,30°$ at $\theta = 1/3$; c(4×2) at $\theta = 1/2$; c($\sqrt{3}\times5$)rect at $\theta = 0.60$; (4$\sqrt{3}\times8$)rect at $\theta = 0.63$; "split (2×2)" at $\theta = 2/3$; and (2×2) at $\theta = 3/4$. Different vibrational frequencies for the C–O stretching modes are observed by IRAS (infrared reflection absorption spectroscopy) corresponding to each coverage[5]: a band appears at 1849 $cm^{-1}$ at $\theta = 1/3$; then shifts to 1918 $cm^{-1}$ at $\theta = 1/2$ and further to 1951 $cm^{-1}$ at $\theta = 0.60$. At higher coverage, a second band appears at 2097 $cm^{-1}$. By comparing with the vibrational frequencies in metal carbonyl clusters, the CO adsorption has been assigned to hollow sites up to $\theta = 1/3$, to bridge sites at $\theta = 1/2$, and to both bridge and atop sites at higher coverages. A dynamical LEED intensity analysis has shown that, at $\theta = 1/3$, CO adsorbs at the fcc-type hollow sites (with no second layer atom directly underneath).[3] The structure models[4] (see Fig. 1) demonstrate a continuous compression of the unit cell of the adsorbate layer until $\theta = 0.60$. Additional CO adsorption causes a hexagonal arrangement. Other alternative structures for $\theta > 0.60$ were also suggested by laser simulation of the LEED patterns.[6]

## II. EXPERIMENTAL

Thermal desorption experiments of CO on Pd(111) were carried out in an ultrahigh vacuum (UHV) system with a background pressure $< 1\times10^{-10}$ Torr, which has

| CO Coverage (ML) | Vibrational Frequency ($cm^{-1}$) | LEED Pattern | Structure Model |
|---|---|---|---|
| 0.33 | 1849 |  |  |
| 0.50 | 1918 |  |  |
| 0.60 | 1951 |  |  |
| 0.63 | 1951<br>2097 |  |  |
| 0.66 | 1951<br>2097 |  |  |
| 0.75 | 1951<br>2097 |  |  |

FIG. 1. CO stretching frequencies, LEED patterns and surface structure models as a function of CO coverage on Pd(111). Results are from Refs. 4 and 5.

 0021-9606/89/116761-06$02.10 © 1989 American Institute of Physics 

been described in detail previously.[7] CO exposure was made through a collimated capillary array molecular beam doser normal to the surface.[8] During temperature programming of the crystal with a constant low heating rate, the desorbing particles were monitored with a differentially pumped and digitized quadrupole mass spectrometer (QMS) in line-of-sight. In this fast pumped UHV system, the QMS signal is directly proportional to the desorption rate. The QMS was located in an apertured shield. The aperture is 1.6 mm in diameter and 2 mm away from the center of the crystal during desorption measurements. This kind of measurement method has been shown to improve the quality of thermal desorption data considerably by elimination of desorption signal from spurious regions of the crystal or its heating leads.[9,10]

The Pd(111) crystal (14.5 mm diameter$\times$1.30 mm thickness) was oriented within $\pm 0.5°$ of the (111) face using the Laue x-ray backreflection technique; it was polished using standard mechanical methods with diamond pastes down to a grain size of 0.25 $\mu$m. The crystal was cleaned rigorously by prolonged cycles of oxygen treatment (1000 K, $\sim 10^{-6}$ Torr), $Ar^+$ bombardment (600 eV, 2 $\mu$A/cm$^2$), and annealing (1200 K). The surface cleanliness was checked by Auger spectroscopy and by the $O_2$-adsorption/CO, $CO_2$-desorption method.[11,12] The clean Pd(111) surface showed a sharp (1$\times$1) LEED pattern. The crystal could be cooled to 87 K using liquid nitrogen and heated to 1300 K resistively. The temperature was measured through a chromel–alumel thermocouple spot welded to the rear edge of the crystal. A linear heating rate (2 K/s) was achieved with a digital programmer.[13]

To avoid the interference of the residual CO (28 amu) in the QMS signal, isotopically labeled $C^{18}O$ (30 amu, MSD isotopes, 97.4% $C^{18}O$) was used instead. This improved the signal-to-noise level significantly in the thermal desorption spectra through reduction of the background signal.

## III. RESULTS

### A. Thermal desorption rate

Thermal desorption measurements for CO on the Pd(111) surface have been performed with various CO exposures (i.e., various initial CO coverages) at two adsorption temperatures, 87 and 200 K. The desorption rate and the CO coverage were calibrated to $\theta_{max} = 0.66$ CO/Pd for saturation at $T_{ads} = 200$ K.

The thermal desorption data are plotted in the form of a three dimensional surface in Figs. 2 and 3. Here one coordinate on the base plane is the surface temperature, while the other coordinate is the surface coverage. During temperature programmed desorption, the CO coverage initially remains constant; at the threshold for desorption, the coverage begins to decrease as ( $-d\theta/dt$) begins to increase. A line in the horizontal $\theta$–$T$ plane joining the threshold desorption points is a plot of the surface coverage vs temperature for a given rate of temperature programming $dT/dt$. The coverage decreases sigmoidally along this line on the figure base and reaches zero near 500 K, where adsorbed CO is no longer stable on the surface in vacuum. The intersection of other horizontal planes with the "surface" yields the curves showing the decrease in surface coverage vs temperature for other constant desorption rates. In addition, from this surface, isothermal curves can be easily obtained by connecting points on "the desorption rate surface" which are at equal temperatures. In fact, projections of the desorption rate surface on the ( $-d\theta/dt$)–$T$ plane are the normal thermal desorption spectra with various initial coverages; and the intersection parallel to the ( $-d\theta/dt$)–$\theta$ plane yields the usual isotherms with various constant temperatures.

THERMAL DESORPTION RATE vs. TEMPERATURE AND COVERAGE

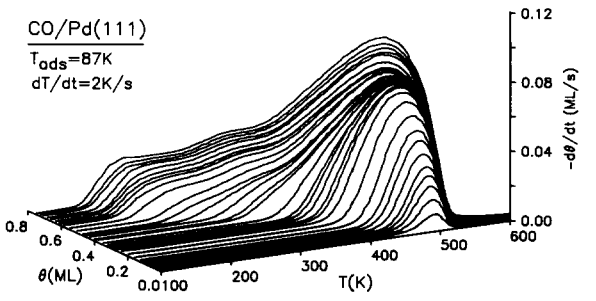


FIG. 2. Thermal desorption rate changes of CO from Pd(111) as a function of surface temperature and surface coverage with various initial coverages. CO adsorption temperature = 87 K.

By comparing the two desorption rate surfaces for different adsorption temperatures (87 and 200 K), the following generalization can be made: (a) At $\theta < 0.3$, the two surfaces are almost identical; (b) at $\theta \approx 0.5$, a second desorption feature shows up for both adsorption temperatures, but for $T_{ads} = 200$ K, this feature continues to grow, whereas for $T_{ads} = 87$ K, a third state starts to appear instead; (c) for $T_{ads} = 200$ K the third state appears at $\theta \geqslant 0.6$ and reaches saturation at $\theta = 0.66$, whereas for $T_{ads} = 87$ K, all three stages grow simultaneously until all are saturated at $\theta = 0.75$. Thus, from this qualitative comparison it can be seen that *the kinetics of desorption in a temperature programmed experiment depend upon the initial temperature and the initial coverage.* Heating during the experiment does not produce equivalent kinetics at equal coverages except at higher temperature and lower coverage.

THERMAL DESORPTION RATE vs. TEMPERATURE AND COVERAGE

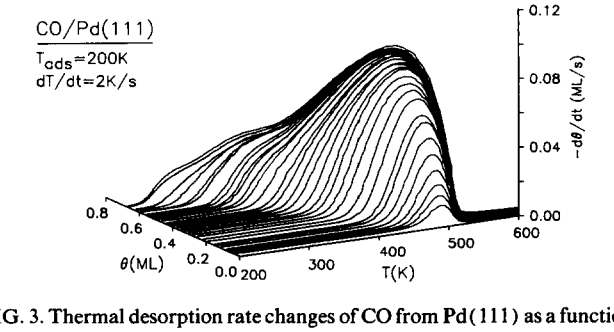


FIG. 3. Thermal desorption rate changes of CO from Pd(111) as a function of surface temperature and surface coverage with various initial coverages. CO adsorption temperature = 200 K.

### B. Desorption activation energy

There exist many procedures to derive the desorption activation energy ($E_d$) and/or preexponential factor ($\nu_n$) from thermal desorption spectra[1,10,14–19] besides the "complete analysis."[20] These procedures fall into two categories: (1) integral approach[1,15,17,19] and (2) differential approach.[10,14,16,18] The integral approach employs the bulk peak characteristics such as temperature at desorption peak maximum,[1] width at half-maximum,[15,17] or partially integrated peak area.[19] These methods are often used to extract coverage-independent kinetic parameters from a single desorption peak. The differential approach uses the desorption rate/temperature data pairs taken from one or more desorption spectra to prepare an Arrhenius-type plot and relates the slope and intercept to $E_d$ and $\nu_n$, respectively. The differential methods can be further divided into two types: one involves the construction of isotherms from a series of desorption spectra,[14,16] another uses the desorption rate/temperature data from the onset of desorption in the low temperature tail (or the threshold region) of a single desorption spectrum.[10,18] Both types of differential methods may be applied to derive coverage-dependent kinetic parameters from a collection of desorption spectra with variable initial coverages, sometimes even for multiple overlapping desorption peaks. Because of its relative ease of application, in this work we choose to use the latter type of method, the threshold temperature programmed desorption (TTPD) method.[10]

Since CO adsorption and desorption on the Pd(111) surface is nondissociative (unity molecularity), we assume that the desorption order is equal to 1 and is constant with coverage.[21] The threshold coverage increments used for all the measurements in this work are below 3% of the initial coverage. In other words, we assume that $E_d$ and $\nu_1$ do not vary significantly within this 3% coverage increment. This assumption will be justified by the linearity of the Arrhenius plots, i.e., the correlation coefficients and variances of the linear regression of the data in the Arrhenius plots.

In Fig. 4, the desorption activation energies at various

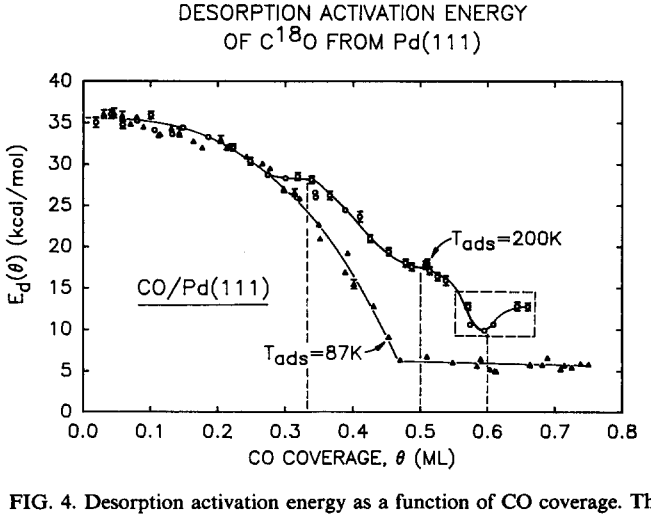


FIG. 4. Desorption activation energy as a function of CO coverage. The error bars are the regression variances of Arrhenius plots. The dashed lines indicate CO coverage = 0.33, 0.50, 0.60 (ML), respectively. Results within the dashed box are shown in separate experiments in Fig. 5, plotted on expanded scales.

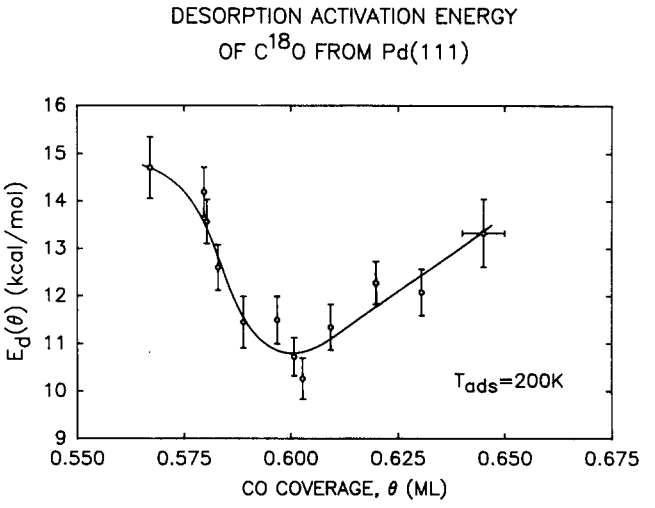


FIG. 5. Desorption activation energy as a function of CO coverage. The error bars are the regression variances of Arrhenius plots. These are additional experiments carried out within the dashed box in Fig. 4. Note the expanded scales.

CO coverages are shown for both adsorption temperatures, 87 and 200 K. The differences are obvious. For $T_{ads} = 200$ K, $E_d = 35.5$ kcal/mol at $\theta = 0$, which agrees reasonably well with the isosteric energy (34 kcal/mol) of CO adsorption on Pd(111) measured by work function changes[22] and with the desorption activation energy (32 kcal/mol) for the same system obtained from modulated molecular beam scattering.[23] As the CO coverage increases, $E_d$ decreases gradually until $\theta \approx 1/3$, where $E_d$ reaches a constant value, 28.5 kcal/mol. A similar plateau appears at $\theta \approx 1/2$ with $E_d = 17.3$ kcal/mol. Then $E_d$ decreases again with increasing coverage and reaches a minimum at $\theta \approx 0.6$. Further CO adsorption at 200 K leads to a small reproducible increase of $E_d$. To confirm this peculiar increase of $E_d(\theta)$, this region of coverage (shown in the dashed box in Fig. 4) was investigated in more detail. The results are plotted in Fig. 5 with expanded scales and fully confirm the small increase in $E_d$ above $\theta = 0.6$. For $T_{ads} = 87$ K, $E_d(\theta)$ follows the curve obtained for $T_{ads} = 200$ K up to $\theta = 0.27$ (see Fig. 4). Above $\theta = 0.27$, $E_d(\theta)$ ($T_{ads} = 87$ K) decreases continuously until $\theta \approx 0.47$. From $\theta \approx 0.47$ to saturation, $E_d$ is almost coverage-independent with a value of $\sim 7$ kcal/mol.

The large difference of $E_d$ at $\theta = 0.5$ between $T_{ads} = 200$ and 87 K lead us to choose this specific coverage and to vary the adsorption temperature. The desorption activation energies at $\theta = 0.50 \pm 0.02$ for variable adsorption temperatures are given in Fig. 6. As can be seen, $E_d$ increases from 87 to 215 K. It should be noted that at these adsorption temperatures and for this coverage, no desorption from the adsorbed states will occur following exposure at the temperatures chosen in the range 87–200 K (cf. Figs. 2 and 3). Interestingly, annealing to 200 K following CO adsorption ($\theta = 0.50$) at 87 K for up to 1800 s increases the desorption activation energy only slightly (less than 2 kcal/mol). This indicates that the differences in CO desorption kinetics are dependent on the temperature of adsorption, and that *annealing* a partially covered CO layer to 200 K is not sufficient

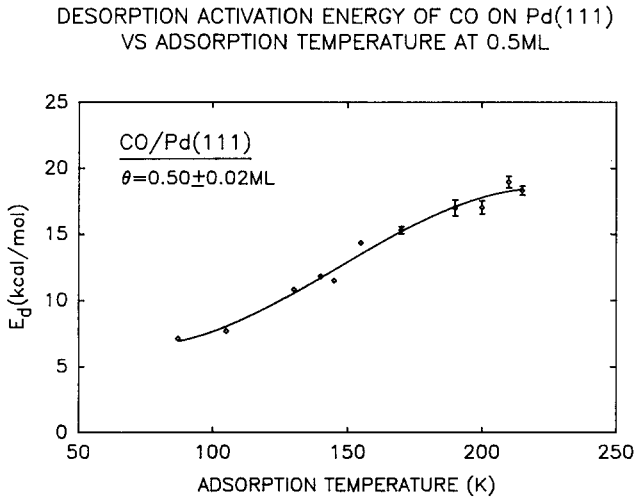


FIG. 6. Adsorption temperature dependence of the desorption activation energy for $\theta = 0.50$ ML. The CO coverage corresponds to the dashed lines of $\theta = 0.5$ ML in Fig. 4.

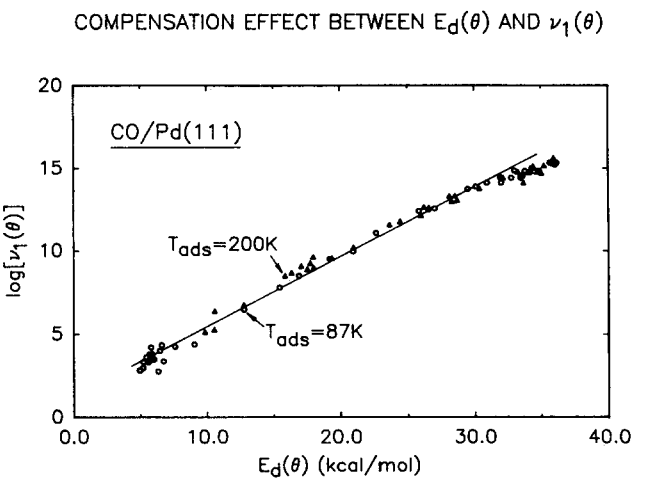


FIG. 8. Compensation effect between desorption activation energy and preexponential factor as a function of coverage [cf. Eq. (2)].

to cause the behavior to resemble a layer *adsorbed* at 200 K. Cooling to 87 K after CO adsorption at 200 K and then programming the temperature gives desorption kinetics with the same kinetic parameters as direct desorption from a CO layer adsorbed at 200 K.

### C. Preexponential factor

The coverage dependence of the preexponential factor is seldom measured because it is often irrationally assumed to be constant. However, the variation of $\nu_n$ with coverage is very useful in describing surface equilibrium and rate processes and in testing the desorption theories.[24] It has been recently concluded,[24] after reviewing ~45 adsorption systems, that among the metal substrates Pd is unusual in that $\nu_n$ rarely changes even when $E_d$ decreases by more than 10 kcal/mol. This is not necessarily correct because there are no desorption kinetic studies in which $\nu_n(\theta)$ is evaluated in the literature for the CO/Pd(111) system [see Ref. 25 for CO/Pd(100)].

Along with the $E_d(\theta)$, $\nu_1(\theta)$ for CO on Pd(111) can also be derived from the thermal desorption spectra (see Figs. 2 and 3) by using the TTPD method.[10] The preexponential factors with variable CO coverages thus derived are shown in Fig. 7. At the limit of $\theta = 0$, $\nu_1 = 10^{15.3}\ s^{-1}$. The minimum value of $\nu_1$ is $10^{2.7}\ s^{-1}$. The preexponential factor varies with coverage by a factor of more than $10^{12}$. This is very different from that of CO on Pd(100)[25] where $\nu_1 \approx 10^{16.5}\ s^{-1}$ and varies very little with coverage. However, the large drop of $\nu$ with coverage is not unusual. Variations of $\nu_1$ with coverage by a factor of $10^6$ are often obtained.[24]

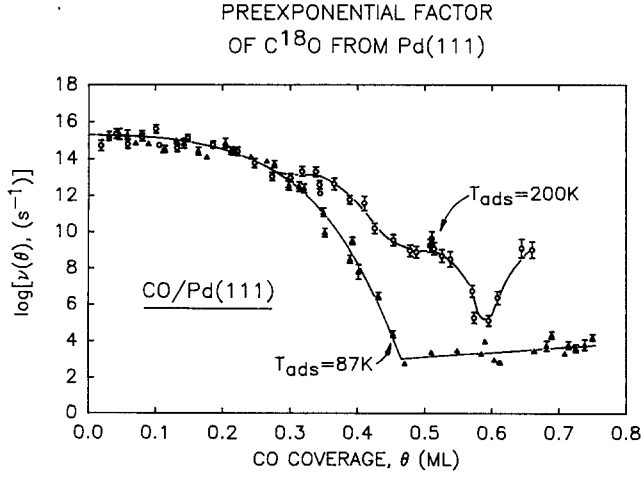


FIG. 7. Preexponential factor for CO desorption as a function of CO coverage. The error bars are the regression variances of Arrhenius plots.

A comparison between $E_d(\theta)$ (Fig. 4) and $\nu_1(\theta)$ (Fig. 7) clearly demonstrates the well-known compensation effect,[26] i.e., the preexponential factor and the desorption activation energy change with coverage following the relationship

$$\ln \nu_1(\theta) = E_d(\theta)/RT_c + c, \qquad (2)$$

where $c$ is a constant, $T_c$ is some characteristic temperature. The plot of $\ln \nu_1(\theta)$ vs $E_d(\theta)$ for CO on Pd(111) gives a nearly straight line (see Fig. 8) with $T_c = 519$ K and $c = 3.0$. The compensation effect is common to most desorption systems.[24] A recent simulation[27] has shown that the compensation effect can drastically influence the desorption spectrum of an adsorbate system with pairwise lateral interactions. It is emphasized[27] that, due to the compensation effect, those desorption analysis procedures based on peak maximum temperature and peak width almost always lead to incorrect results except possibly in the limit of zero coverage.[28] According to the simulation, $T_c = 519$ K as we obtained here, indicates a relatively strong compensation effect. Therefore, it is very reasonable to use the TTPD analysis procedure[10] as we have done.

## IV. DISCUSSION

### A. Precursor influence and nonequilibrium effect

Until this point, we have implicitly assumed that the conventional Polanyi–Wigner equation [Eq. (1)] is a good model for thermal desorption with the modification of coverage dependent $E_d$ and $\nu_n$ to account for lateral interactions. Rigorously speaking, this model with the modification

applies only for direct desorption, i.e., desorption without going through an intermediate state (precursor state). The cosine angular scattering distribution and the nonlinear decrease of sticking coefficient with coverage[23] indicate that CO adsorption on Pd(111) is precursor mediated (intrinsically and extrinsically). From the detailed balancing principle (microscopic reversibility), the desorption process of CO from Pd(111) should be a precursor-mediated one. Due to the possible influence of precursor states, what we have derived from the desorption spectra can only be safely considered as *effective* desorption kinetic parameters.

There have been several attempts to write a desorption rate expression accounting for the precursor influence.[29–31] Unfortunately, these kinds of expressions, not to mention the assumptions to be justified, are rather complicated and contain several adjustable parameters for curve fitting. Nevertheless, some physical pictures can be provided by these expressions.

Another effect which might influence even the effective desorption parameters is the nonequilibrium factor. A recent simulation[32] has shown a dramatic influence of nonequilibrium island-forming adlayers on the desorption kinetics. It also demonstrates[32] that the influence strongly depends on heating rate and attractive lateral interactions. However, a comparison of the desorption kinetic parameters for CO on Ru(001) obtained from thermal desorption spectra and from (close to) equilibrium measurements shows no significant influence of nonequilibrium effects on the results.[33] But, the situation of CO on Pd(111) might be different from that of CO on Ru(001).

### B. Correlation of $E_d$ with surface phase transitions

Although the effective desorption activation energy ($E_d$) may not be equal to the binding energy due to the effects just discussed above, the correlation of $E_d(\theta)$ at $T_{ads} = 200$ K (Fig. 4) with LEED patterns (Fig. 1) is still very interesting, which may in turn suggest that $E_d(T_{ads} = 200\ \text{K})$ is proportional, if not equal, to the binding energy.

As we have seen in Fig. 4, $E_d(\theta)$ ($T_{ads} = 200$ K) approaches its first plateau at $\theta \approx 1/3$ (see the dashed line) where a $(\sqrt{3}\times\sqrt{3})R\ 30°$ LEED pattern develops fully. A similar behavior of isosteric adsorption energy with coverage was also observed previously for the same system.[22] As the coverage increases, the adsorbate unit cell compresses leading to a gradual drop of $E_d$, which is probably due to the increasing repulsive lateral interactions. When a stable $c(4\times2)$ structure forms, $E_d$ stops decreasing as shown by the short plateau at $\theta = 0.5$ (Fig. 4). Further compression of the $c(4\times2)$ unit cell causes $E_d$ to decrease again. At $\theta \approx 0.60$, the unit cell reaches its minimum dimension; so does $E_d$, indicating that relatively strong repulsive lateral interactions exist among adsorbates. Additional CO adsorption changes the adlayer to a hexagonal structure with a fraction of the CO species adsorbed terminally on the top of Pd atoms. This arrangement apparently relaxes the strong repulsive lateral interactions, and $E_d$ starts to *increase* with coverage (see Figs. 4 and 5).

This four-stage correlation between $E_d$ and phase transition has not been reported previously for CO adsorption. There have been observations of one- or two-stage correlations: the binding energy of CO on Pd(100) drops by 8 kcal/mol when a $c(4\times2)R\ 45°$ LEED pattern is observed[34]; the isosteric heat of adsorption of CO on Ni(111) decreases from 26.5 to 23.5 kcal/mol at $\theta = 1/3$ corresponding to the formation of a $(\sqrt{3}\times\sqrt{3})R\ 30°$ structure[35]; for CO on Co(0001), the isosteric heat of adsorption drops from a constant value of 31 to ~23 kcal/mol coinciding with the transition from $(\sqrt{3}\times\sqrt{3})R\ 30°$ to $(2\sqrt{3}\times2\sqrt{3})R\ 30°$ structures.[36] This kind of correlation is not unexpected. In principle, the coverage-dependent desorption activation energy, as a microscopic average, should reflect the changes of adsorbate structure which are a result of lateral interactions. This is clearly demonstrated by our observations.

### C. Adsorption temperature dependence of $E_d$

In Fig. 4, we have shown the different behavior of $E_d$ with coverage due to the different adsorption temperatures. The adsorption temperature dependence of $E_d(\theta = 0.50)$ has been shown in Fig. 6. Since the desorption peak shapes also show differences correspondingly (cf. Figs. 2 and 3), the differences in $E_d$ are real and are not due to the data analysis method used. Neither is it likely due to a possibly different precursor effect on $E_d(T_{ads})$. Therefore, phenomenologically speaking, the memory of the adsorption temperature kept in the desorption rate (which governs the effective desorption activation energy) must suggest a nonequilibrium effect.

What could then account for this strong nonequilibrium effect? One possible answer is the formation of domains. A time-dependent Monte Carlo simulation for $N_2$ on Ru(001) has demonstrated[37] the interrelationship between desorption kinetics and domain formation. As the surface temperature increases, desorption proceeds first from antiphase domains, then from domain boundaries. As the domains become smaller, the desorption activation energy barrier becomes higher. This suggests that desorption from isolated small domains would show a high effective desorption activation energy. Knowing this relationship, we could presume that, *during adsorption* of CO on Pd(111), the adsorbate would form many small domains at $T_{ads} = 200$ K. This would form a highly defective overlayer at this elevated temperature of adsorption. In contrast, fewer large domains would form at $T_{ads} = 87$ K, and an intermediate number of intermediate size domains would form at intermediate adsorption temperatures, i.e., the tendency to form defective structures during adsorption would be less at lower temperatures. Domain size and number would be difficult, if not impossible, to be significantly varied by cooling, heating or annealing within a certain temperature range for higher coverages due to the tendency to form interlocked structures. This would explain the adsorption temperature dependence of the effective desorption activation energy. The tendency to form interlocked domains during adsorption should occur mainly at higher coverages; hence, we see no adsorption temperature effect on $E_d$ or $\nu$ below $\theta = 0.27$ (Figs. 4 and 7).

The justification of these assumptions must await further experiments and simulations, but some experimental

observations supporting the assumptions are already available. The IRAS and LEED studies[5] have shown that, at 300 K, the CO stretching band appears at constant frequency as a function of coverage below $\theta = 1/3$, and the $(\sqrt{3}\times\sqrt{3})R$ 30° structure is observed over an extended coverage range. This indicates the formation and growth of small islands at 300 K, which may be similar at 200 K. At 90 K, however, the CO stretching band gradually shifts to higher frequency (from 1808 to 1849 $cm^{-1}$) as the coverage increases, and at $\theta = 1/3$ the $\sqrt{3}$ spots in LEED and the IR band are much sharper,[5] suggesting that a better ordered, larger domain structure is completed.

From an 87 K-adsorption experiment, the ~2 kcal/mol increase of $E_d$ due to annealing at 200 K for 1800 s and the small effect on $E_d$ by cooling from 200 to 87 K indicate that annealing may slowly break a large domain into small domains, but cooling cannot merge several small domains. This behavior is thermodynamically and kinetically reasonable.

A similar adsorption temperature dependence of $E_d$ was also observed previously in our laboratory for CO on Ni(111).[10] Thus phenomena of this type may be of general importance.

## V. SUMMARY

The following results have been obtained from the thermal desorption study of CO on the Pd(111) surface:

(1) The effective desorption activation energy at zero coverage is 35.5 kcal/mol, independent of the adsorption temperature from 87 to 200 K.

(2) A four-stage correlation between $E_d(\theta)$ ($T_{ads} = 200$ K) and the development of stable LEED structures as a function of coverage has been observed, including an unusual increase of $E_d$ with coverage for $\theta > 0.60$.

(3) The preexponential factor at zero coverage is $10^{15.3}$ $s^{-1}$. A strong compensation effect between $E_d$ and $\nu_1$ with $T_c = 519$ K has been observed.

(4) The dependence of $E_d$ on adsorption temperature has been examined and interpreted qualitatively using a model involving the formation of domains whose size governs the desorption kinetics. Annealing experiments indicate that non-equilibrium surface structures are present during desorption in the coverage range above ~0.25 CO/Pd.

## ACKNOWLEDGMENT

The support of this work by the Army Research Office (Contract No. DAAL-03-89-K-0005) is gratefully acknowledged.

[1] P. A. Redhead, Vacuum **12**, 203 (1962).
[2] J. T. Yates, Jr., in *Methods of Experimental Physics*, edoted by R. L. Park and M. G. Lagally (Academic, New York, 1985), Vol. 22, Chap. 8.
[3] H. Ohtani, M. A. Van Hove, and G. A. Somorjai, Surf. Sci. **187**, 372 (1987), and references therein.
[4] H. Conrad, G. Ertl, and J. Küppers, Surf. Sci. **76**, 323 (1978).
[5] F. M. Hoffmann, Surf. Sci. Rep. **3**, 107 (1983).
[6] J. P. Biberian and M. A. Van Hove, Surf. Sci. **138**, 361 (1984).
[7] S. M. Gates, J. N. Russell, Jr., and J. T. Yates, Jr., Surf. Sci. **159**, 233 (1985).
[8] M. J. Bozack, L. Muehlhoff, J. N. Russell, Jr., W. J. Choyke, and J. T. Yates, Jr., J. Vac. Sci. Technol. A **5**, 1 (1987).
[9] P. Feulner and D. Menzel, J. Vac. Sci. Technol. **17**, 662 (1980).
[10] J. B. Miller, H. R. Siddiqui, S. M. Gates, J. N. Russell, Jr., J. T. Yates, Jr., J. C. Tully, and M. J. Cardillo, J. Chem. Phys. **87**, 6725 (1987).
[11] H. Conrad, G. Ertl, J. Küppers, and E. E. Latta, Surf. Sci. **65**, 245 (1977).
[12] M. Grunze, H. Ruppender, and O. Elshazly, J. Vac. Sci. Technol. A **6**, 1266 (1988).
[13] R. J. Muha, S. M. Gates, J. T. Yates, Jr., and P. Basu, Rev. Sci. Instrum. **56**, 613 (1985).
[14] E. Bauer, H. Poppa, G. Todd, and F. Bonczek, J. Appl. Phys. **45**, 5164 (1974).
[15] D. Edwards, Jr., Surf. Sci. **54**, 1 (1976).
[16] J. L. Falconer and R. J. Madix, J. Catal. **48**, 262 (1977).
[17] C.-M. Chan, R. Aris, and W. H. Weinberg, Appl. Surf. Sci. **1**, 360 (1978).
[18] E. Habenschaden and J. Küppers, Surf. Sci. **138**, L147 (1984).
[19] E. Tronconi and L. Lietti, Surf. Sci. **199**, 43 (1988).
[20] D. A. King, Surf. Sci. **47**, 384 (1975).
[21] D. Menzel, in *Chemistry and Physics of Solid Surfaces IV*, edited by R. Vanselow and R. Howe (Springer, Berlin, 1982), p. 389.
[22] G. Ertl and J. Koch, Z. Naturforsch. Teil A **25**, 1906 (1970).
[23] T. Engel, J. Chem. Phys. **69**, 373 (1978).
[24] E. G. Seebauer, A. C. F. Kong, and L. D. Schmidt, Surf. Sci. **193**, 417 (1988).
[25] R. J. Behm, K. Christmann, and G. Ertl, J. Chem. Phys. **73**, 2984 (1980).
[26] G. C. Bond, *Catalysis by Metals* (Academic, London, 1962), p. 139.
[27] J. W. Niemantsverdriet, K. Markert, and K. Wandelt, Appl. Surf. Sci. **31**, 211 (1988); J. W. Niemantsverdriet and K. Wandelt, J. Vac. Sci. Technol. A **6**, 757 (1988).
[28] J. T. Yates, Jr., P.A. Thiel, and W. H. Weinberg, Surf. Sci. **84**, 427 (1979).
[29] D. A. King, Surf. Sci. **64**, 43 (1977).
[30] R. Gorte and L. D. Schmidt, Surf. Sci. **76**, 559 (1978).
[31] A. Cassuto and D. A. King, Surf. Sci. **102**, 388 (1981).
[32] J. W. Evans and H. Pak, Surf. Sci. **199**, 28 (1988).
[33] H. Pfnür, P. Feulner, and D. Menzel, J. Chem. Phys. **79**, 4613 (1983).
[34] J. C. Tracy and P.W. Palmberg, J. Chem. Phys. **51**, 4852 (1969).
[35] K. Christmann, O. Schober, and G. Ertl, J. Chem. Phys. **60**, 4719 (1974).
[36] H. Papp, Surf. Sci. **129**, 205 (1983).
[37] E. S. Hood, B. H. Toby, and W. H. Weinberg, Phys. Rev. Lett. **55**, 2437 (1985).